Direction Finding With Partly Calibrated Uniform Linear Arrays

Bin Liao, *Student Member, IEEE*, and Shing Chow Chan, *Member, IEEE*

***Abstract*—A new method for direction finding with partly calibrated uniform linear arrays (ULAs) is presented. It is based on the conventional estimation of signal parameters via rotational invariance techniques (ESPRIT) by modeling the imperfections of the ULAs as gain and phase uncertainties. For a fully calibrated array, it reduces to the conventional ESPRIT algorithm. Moreover, the direction-of-arrivals (DOAs), unknown gains, and phases of the uncalibrated sensors can be estimated in closed form without performing a spectral search. Hence, it is computationally very attractive. The Cramér–Rao bounds (CRBs) of the partly calibrated ULAs are also given. Simulation results show that the root mean squared error (RMSE) performance of the proposed algorithm is better than the conventional methods when the number of uncalibrated sensors is large. It also achieves satisfactory performance even at low signal-to-noise ratios (SNRs).**

***Index Terms*—Direction-of-arrival (DOA), estimation of signal parameters via rotational invariance techniques (ESPRIT), partly calibrated arrays, uniform linear array (ULA).**

I. Introduction

SENSOR array processing using antenna arrays has been successfully applied to many engineering fields including wireless communications and radar systems. In particular, the theoretical as well as applied aspects of direction finding have received great research interest during the last decades [1], [2]. Given an ideal antenna array without any uncertainties, direction-of-arrivals (DOAs) can be estimated with high accuracy using high- or super-resolution methods such as multiple signal classification (MUSIC) [3], root-MUSIC [4], estimation of signal parameters via rotational invariance techniques (ESPRIT) [5], and maximum likelihood (ML) algorithm [6]. However, antenna arrays in practice usually suffer from imperfections such as unknown or misspecified mutual coupling, imperfectly known sensor positions and orientations, gain, and phase imbalances [2].

It has been shown that conventional high- or super-resolution direction finding techniques are sensitive to array model errors, which will considerably degrade the performance of these techniques [2], [7]–[9]. A number of calibration methods have been proposed to deal with these problems, and the performances of conventional methods may be significantly improved by taking these antenna array uncertainties into account [10]–[16]. Theoretically, fully calibrated antenna arrays are preferred since high- or super-resolution direction finding techniques can be applied directly. Nevertheless, antenna arrays in some practical applications may be incompletely calibrated. Hence, the response of some sensor elements is poorly known or even unknown. This class of arrays is usually referred to as *partly calibrated* arrays, and a number of DOA estimation methods have been devoted to these arrays [17]–[24]. For instance, direction finding with partly calibrated arrays was addressed in [18] using the ML algorithm. This method requires the number of calibrated sensors to be larger than the number of signals. In [19], an algorithm for estimating the DOAs and the gains and phases of the uncalibrated sensors was proposed by minimizing a certain cost function. It has been shown that this method can achieve a satisfactory performance. However, due to the requirement of line searches and iterations, its complexity may be high, and the convergence to the global minimum cannot be guaranteed [19]. More recently, the approach in [20] extended the ML criterion used in fully calibrated arrays and employed a particle swarm optimization (PSO) algorithm to solve the problem of direction finding in partly calibrated arrays. Simulation results showed that it has a better performance than the approach in [19]. However, its complexity is high because the searching process is random in nature.

In addition, the problem of DOA estimation using partly calibrated arrays containing multiple subarrays has been studied [21]–[24]. This is of great interest since in large subarray-based systems, it may be difficult to calibrate the whole array, though each subarray can be well calibrated [17]. A well-known class of methods is the rank-reduction (RARE) estimator proposed in [21]–[24]. The root-RARE algorithm in [21] and [22] is computationally efficient, but the subarrays are required to be linear identically oriented, and the interelement spacings should be integer multiples of a known shortest baseline. For more general cases where the geometries of subarrays are arbitrary, a spectral-RARE algorithm was proposed in [23] and [24]. However, the sensor number M, subarray number K, and source number L have to satisfy the condition $K \leq M - L$. Compared to the root-RARE algorithm, the complexity will be higher since an additional one-dimensional spectral search is needed. It is worth noting that although RARE algorithms are based on multiple subarrays, their applications to some common arrays such as uniform linear arrays (ULAs) are straightforward. However, there may exist some limitations when these methods are applied to ULAs, as we will show later in Section IV.

Manuscript received February 25, 2011; revised June 22, 2011; accepted July 28, 2011. Date of publication October 21, 2011; date of current version February 03, 2012.

The authors are with the Department of Electrical and Electronic Engineering, The University of Hong Kong, Hong Kong (e-mail: liaobin@eee.hku.hk; scchan@eee.hku.hk).

Color versions of one or more of the figures in this paper are available online at http://ieeexplore.ieee.org.

Digital Object Identifier 10.1109/TAP.2011.2173144

In this paper, we consider the problem of direction finding with partly calibrated ULAs, which occurs in a number of practical applications [17]–[20]. A simple but efficient method based on the conventional ESPRIT algorithm is proposed. It is well known that the conventional ESPRIT algorithm generally requires the array to be fully calibrated and the subarrys be identically oriented. Unfortunately, as mentioned, the arrays available in practice may only be partly calibrated, and hence the ESPRIT algorithm is not directly applicable. In this study, the array manifold of the partly calibrated ULAs is modeled so that the conventional ESPRIT algorithm can be extended to this class of arrays by taking the imperfections into account. The proposed method does not require any spectral search, and the DOAs as well as the gains and phases can be jointly estimated in closed form.

The rest of this paper is organized as follows. The models of ideal and partly calibrated ULAs are first introduced in Section II. The proposed method for DOA estimation using partly calibrated ULAs is presented in Section III. An analysis of the proposed method and the Cramér–Rao bounds (CRBs) of the partly calibrated ULAs are given in Section IV. Numerical examples are conducted in Section V to evaluate the performance of the proposed method. Finally, Section VI concludes the paper.

II. Array Models

A. Ideal ULA Model

To begin with, we consider an ideal ULA with M isotropic sensors impinged by L uncorrelated narrowband source signals, $\{s_l(t)\}_{l=1}^{L}$, from far field. The array output observed at the tth snapshot consists of the outputs of the M sensors and can be written as

$$\boldsymbol{x}(t) = \sum_{l=1}^{L} \boldsymbol{a}(\theta_l)s_l(t) + \boldsymbol{n}(t) = \boldsymbol{A}\boldsymbol{s}(t) + \boldsymbol{n}(t) \tag{1}$$

where $\boldsymbol{a}(\theta_l)$ is the $M \times 1$ steering vector corresponding to the DOA of the lth source, i.e., θ_l, and the array geometry, $\boldsymbol{A}$ is the $M \times L$ steering matrix

$$\boldsymbol{A} = [\boldsymbol{a}(\theta_1), \boldsymbol{a}(\theta_2), \ldots, \boldsymbol{a}(\theta_L)] \tag{2}$$

$\boldsymbol{s}(t) = [s_1(t), s_2(t), \ldots, s_L(t)]^T$ is the $L \times 1$ vector of the signal waveforms, and $\boldsymbol{n}(t)$ is the $M \times 1$ sensor noise vector that is commonly assumed to be additive white Gaussian noise (AWGN) vector with zero mean and covariance matrix $\sigma^2\boldsymbol{I}$, where σ^2 and $\boldsymbol{I}$ denote the noise variance and $M \times M$ identity matrix, respectively. For the cases of ideal ULAs, the steering vector is given by

$$\boldsymbol{a}(\theta) = [1, e^{j2\pi\lambda^{-1}d\sin\theta}, \ldots, e^{j2\pi\lambda^{-1}(M-1)d\sin\theta}]^T \tag{3}$$

with λ, d, and θ denoting the carrier wavelength, intersensor spacing, and DOA, respectively. From (1), the array covariance matrix of the array output is

$$\boldsymbol{R} = E\{\boldsymbol{x}(t)\boldsymbol{x}^H(t)\} = \boldsymbol{A}\boldsymbol{S}\boldsymbol{A}^H + \sigma^2\boldsymbol{I} \tag{4}$$

where $\boldsymbol{S} = E\{\boldsymbol{s}(t)\boldsymbol{s}^H(t)\}$ is the signal covariance matrix, and $E\{\cdot\}$ denotes the statistic expectation.

B. Partly Calibrated ULA Model

We now consider the case where only part of the ULA is calibrated. Without loss of generality, it is assumed that the first M_{c} sensors of the array are calibrated, whereas the last $M - M_{\mathrm{c}}$ sensors are uncalibrated with uncertainties modeled as unknown, direction-independent gains and phases. Let $\boldsymbol{\rho}$ and $\boldsymbol{\varphi}$ represent the $M \times 1$ array gain and phase vectors, respectively. Then, we have

$$\boldsymbol{\rho} = [\boldsymbol{1}_{M_{\mathrm{c}}}^T, \rho_1, \ldots, \rho_{M-M_{\mathrm{c}}}]^T \tag{5a}$$

$$\boldsymbol{\varphi} = [\boldsymbol{1}_{M_{\mathrm{c}}}^T, e^{j\varphi_1}, \ldots, e^{j\varphi_{M-M_{\mathrm{c}}}}]^T \tag{5b}$$

where $\boldsymbol{1}_{M_{\mathrm{c}}}$ denotes an $M_{\mathrm{c}} \times 1$ vector with all elements equal to one, and $\rho_1, \ldots, \rho_{M-M_{\mathrm{c}}}$ and $\varphi_1, \ldots, \varphi_{M-M_{\mathrm{c}}}$ are the unknown sensor gains and phases of the uncalibrated $M - M_{\mathrm{c}}$ sensors, respectively. Taking these unknown uncertainties into account, the steering vector of the partly calibrated ULAs can be written as

$$\overline{\boldsymbol{a}}(\theta) = \boldsymbol{\Gamma}(\boldsymbol{\gamma})\boldsymbol{a}(\theta) = \boldsymbol{\Gamma}(\boldsymbol{\rho} \circ \boldsymbol{\varphi})\boldsymbol{a}(\theta) \tag{6}$$

where $\circ$ denotes the Schur–Hadamard product

$$\boldsymbol{\gamma} = \boldsymbol{\rho} \circ \boldsymbol{\varphi} = [\boldsymbol{1}_{M_{\mathrm{c}}}^T, \rho_1 e^{j\varphi_1}, \ldots, \rho_{M-M_{\mathrm{c}}} e^{j\varphi_{M-M_{\mathrm{c}}}}]^T \tag{7}$$

and $\boldsymbol{\Gamma}(\boldsymbol{\gamma}) = \mathrm{diag}\{\gamma_1, \gamma_2, \ldots, \gamma_M\}$ is an $M \times M$ diagonal matrix. Hence, the array covariance matrix becomes

$$\boldsymbol{R} = \overline{\boldsymbol{A}}\boldsymbol{S}\overline{\boldsymbol{A}}^H + \sigma^2\boldsymbol{I} = \boldsymbol{\Gamma}(\boldsymbol{\gamma})\boldsymbol{A}\boldsymbol{S}\boldsymbol{A}^H\boldsymbol{\Gamma}^H(\boldsymbol{\gamma}) + \sigma^2\boldsymbol{I} \tag{8}$$

where $\overline{\boldsymbol{A}} = \boldsymbol{\Gamma}(\boldsymbol{\gamma})\boldsymbol{A}$ is the steering matrix of the partly calibrated ULA. The eigenvalue decomposition (EVD) of (8) can be written as

$$\boldsymbol{R} = \boldsymbol{E}_{\mathrm{S}}\boldsymbol{\Lambda}_{\mathrm{S}}\boldsymbol{E}_{\mathrm{S}}^H + \boldsymbol{E}_{\mathrm{N}}\boldsymbol{\Lambda}_{\mathrm{N}}\boldsymbol{E}_{\mathrm{N}}^H \tag{9}$$

where $\boldsymbol{\Lambda}_{\mathrm{S}}$ is an $L \times L$ diagonal matrix consisting of L largest eigenvalues and $\boldsymbol{\Lambda}_{\mathrm{N}}$ is an $(M-L) \times (M-L)$ diagonal matrix consisting of $M - L$ smallest eigenvalues. $\boldsymbol{E}_{\mathrm{S}}$ is the $M \times L$ signal subspace matrix containing the L eigenvectors with the L largest eigenvalues, while $\boldsymbol{E}_{\mathrm{N}}$ is the $M \times (M-L)$ noise subspace matrix containing the $M - L$ eigenvectors with the $M - L$ smallest eigenvalues. In cases of finite snapshots, the array covariance matrix and its EVD can be computed as $\hat{\boldsymbol{R}} = N^{-1}\sum_{t=1}^{N}\boldsymbol{x}(t)\boldsymbol{x}^H(t) = \hat{\boldsymbol{E}}_{\mathrm{S}}\hat{\boldsymbol{\Lambda}}_{\mathrm{S}}\hat{\boldsymbol{E}}_{\mathrm{S}}^H + \hat{\boldsymbol{E}}_{\mathrm{N}}\hat{\boldsymbol{\Lambda}}_{\mathrm{N}}\hat{\boldsymbol{E}}_{\mathrm{N}}^H$, where N is the total number of snapshots. The problem we are interested in is to estimate the DOAs $\{\theta_l\}_{l=1}^{L}$ as well as the unknown gains $\{\rho_k\}_{k=1}^{M-M_{\mathrm{c}}}$ and phases $\{\varphi_k\}_{k=1}^{M-M_{\mathrm{c}}}$ from array observations.

III. DOA Estimation

We now proceed to estimate the DOAs as well as the unknown gains and phases of the partly calibrated ULAs. Similar to the conventional ESPRIT algorithm, we divide the partly calibrated ULA into two overlapping subarrays. The first one

comprises the first $M-1$ sensors, while the second one comprises the last $M-1$ sensors. The steering matrices of these two subarrays can be written as

$$\overline{\boldsymbol{A}}_1 = \boldsymbol{\Gamma}(\boldsymbol{\gamma}_1)\boldsymbol{A}_1 \tag{10a}$$
$$\overline{\boldsymbol{A}}_2 = \boldsymbol{\Gamma}(\boldsymbol{\gamma}_2)\boldsymbol{A}_2 \tag{10b}$$

where $\boldsymbol{A}_1$ and $\boldsymbol{A}_2$ denote the nominal steering matrices of the subarrays, and they are equivalent to the first $M-1$ rows and last $M-1$ rows of $\boldsymbol{A}$, respectively. $\boldsymbol{\gamma}_1$ and $\boldsymbol{\gamma}_2$ denote the $(M-1)\times 1$ gain and phase vectors of these two subarrays, and

$$\boldsymbol{\gamma}_1 = [\mathbf{1}_{M_c}^T, \rho_1 e^{j\varphi_1}, \ldots, \rho_{M-M_c-1} e^{j\varphi_{M-M_c-1}}]^T \tag{11a}$$
$$\boldsymbol{\gamma}_2 = [\mathbf{1}_{M_c-1}^T, \rho_1 e^{j\varphi_1}, \ldots, \rho_{M-M_c} e^{j\varphi_{M-M_c}}]^T. \tag{11b}$$

It can also be noted that $\boldsymbol{A}_1$ and $\boldsymbol{A}_2$ satisfy

$$\boldsymbol{A}_2 = \boldsymbol{A}_1\boldsymbol{\Phi} \tag{12}$$

where $\boldsymbol{\Phi}$ is an $L \times L$ diagonal matrix of the phase delays of the first and second subarrays for the L sources, and it is given by

$$\boldsymbol{\Phi} = diag\{e^{j2\pi\lambda^{-1}d\sin\theta_1}, e^{j2\pi\lambda^{-1}d\sin\theta_2} \ldots, e^{j2\pi\lambda^{-1}d\sin\theta_L}\}. \tag{13}$$

Since the signal subspace $\boldsymbol{E}_{\mathrm{S}}$ spans the same space as the steering matrix $\boldsymbol{\Gamma}(\boldsymbol{\gamma})\boldsymbol{A}$, i.e., $\mathrm{span}\{\boldsymbol{E}_{\mathrm{S}}\} = \mathrm{span}\{\boldsymbol{\Gamma}(\boldsymbol{\gamma})\boldsymbol{A}\}$, there exists an $L \times L$ nonsingular matrix $\boldsymbol{T}$ satisfying

$$\boldsymbol{E}_{\mathrm{S}} = \boldsymbol{\Gamma}(\boldsymbol{\gamma})\boldsymbol{A}\boldsymbol{T}. \tag{14}$$

Inspired by the conventional ESPRIT algorithm, let $\boldsymbol{E}_{\mathrm{S}_1}$ consist of the first $M-1$ rows of $\boldsymbol{E}_{\mathrm{S}}$ and represent the signal subspace of the first subarray, and $\boldsymbol{E}_{\mathrm{S}_2}$ consist of the last $M-1$ rows of and represent the signal subspace of the second subarray. Consequently, we have

$$\boldsymbol{E}_{\mathrm{S}_1} = \boldsymbol{\Gamma}(\boldsymbol{\gamma}_1)\boldsymbol{A}_1\boldsymbol{T} \tag{15a}$$
$$\boldsymbol{E}_{\mathrm{S}_2} = \boldsymbol{\Gamma}(\boldsymbol{\gamma}_2)\boldsymbol{A}_2\boldsymbol{T}. \tag{15b}$$

Since the matrices $\boldsymbol{\Gamma}(\boldsymbol{\gamma}_1), \boldsymbol{\Gamma}(\boldsymbol{\gamma}_2)$, and $\boldsymbol{T}$ are nonsingular, one can substitute (12) into (15) and get

$$\boldsymbol{\Gamma}(\overline{\boldsymbol{\gamma}})\boldsymbol{E}_{\mathrm{S}_2} = \boldsymbol{E}_{\mathrm{S}_1}\boldsymbol{\Psi} \tag{16}$$

where the $L \times L$ matrix $\boldsymbol{\Psi}$ is given by

$$\boldsymbol{\Psi} = \boldsymbol{T}^{-1}\boldsymbol{\Phi}\boldsymbol{T} \tag{17}$$

and $\boldsymbol{\Gamma}(\overline{\boldsymbol{\gamma}}) = \boldsymbol{\Gamma}(\boldsymbol{\gamma}_1)\boldsymbol{\Gamma}^{-1}(\boldsymbol{\gamma}_2) = \mathrm{diag}\{\overline{\gamma}_1, \overline{\gamma}_2, \ldots, \overline{\gamma}_{M-1}\}$ with $\overline{\boldsymbol{\gamma}}$ being an $(M-1)\times 1$ vector as

$$\overline{\boldsymbol{\gamma}} = [\mathbf{1}_{M_c-1}^T, \rho_1^{-1}e^{-j\varphi_1}, \rho_1\rho_2^{-1}e^{-j(\varphi_2-\varphi_1)}, \ldots, \rho_{M-M_c-1}\rho_{M-M_c}^{-1}e^{-j(\varphi_{M-M_c}-\varphi_{M-M_c-1})}]^T. \tag{18}$$

Here, we note that the first M_c-1 elements of $\overline{\boldsymbol{\gamma}}$ are equal to one, i.e., $\overline{\gamma}_i = 1, i = 1, 2, \ldots, M_c - 1$. It can be found in (17) that $\boldsymbol{\Psi}$ and $\boldsymbol{\Phi}$ are *similar matrices*. Therefore, the eigenvalues of $\boldsymbol{\Psi}$ must be equal to the diagonal elements of $\boldsymbol{\Phi}$, and the columns of $\boldsymbol{T}$ are the eigenvectors of $\boldsymbol{\Psi}$ [5]. In order to show the relationship between $\boldsymbol{\Psi}$, the DOAs, and the unknown gains and phases of the partly calibrated ULA, we let $v_1, v_2, \ldots, v_L$ be the L eigenvalues of $\boldsymbol{\Psi}$. Hence, the DOAs can be estimated as

$$\theta_l = \sin^{-1}\left\{\frac{\lambda \arg(v_l)}{2\pi d}\right\} \tag{19}$$

where $l = 1, 2, \ldots, L$. Furthermore, given the vector $\overline{\boldsymbol{\gamma}}$ in (18), the unknown gains and phases can be obtained as

$$\rho_k e^{j\varphi_k} = \left(\prod_{i=M_c-1}^{M_c-1+k} \overline{\gamma}_i\right)^{-1} \tag{20}$$

where $k = 1, 2, \ldots, M - M_c$.

Since $\boldsymbol{\Psi}$ and $\overline{\boldsymbol{\gamma}}$ are still unknown, we propose to estimate them in the finite samples case according to (16) and (18) by solving the following optimization problem:

$$\begin{aligned} \min_{\boldsymbol{\Psi},\overline{\boldsymbol{\gamma}}} \quad & ||\boldsymbol{\Gamma}(\overline{\gamma})\hat{\boldsymbol{E}}_{\mathrm{S}_2} - \hat{\boldsymbol{E}}_{\mathrm{S}_1}\boldsymbol{\Psi}||_{\mathrm{F}}^2 \\ \text{s. t.} \quad & \overline{\gamma}_i = 1, i = 1, 2, \ldots, M_c - 1, \end{aligned} \tag{21}$$

where $||\cdot||_{\mathrm{F}}$ denotes the Frobenius norm. In order to solve this problem, we first minimize the objective function with respect to $\boldsymbol{\Psi}$. This gives the least squares solution as follows:

$$\hat{\boldsymbol{\Psi}} = (\hat{\boldsymbol{E}}_{\mathrm{S}_1}^H\hat{\boldsymbol{E}}_{\mathrm{S}_1})^{-1}\hat{\boldsymbol{E}}_{\mathrm{S}_1}^H\boldsymbol{\Gamma}(\overline{\boldsymbol{\gamma}})\hat{\boldsymbol{E}}_{\mathrm{S}_2}. \tag{22}$$

Substitute this back to (21), and after some manipulation as shown in the Appendix, the problem in (21) can be finally reformulated as

$$\begin{aligned} \min_{\overline{\boldsymbol{\gamma}}} \quad & \overline{\boldsymbol{\gamma}}^H\boldsymbol{Q}\overline{\boldsymbol{\gamma}} \\ \text{s. t.} \quad & \overline{\gamma}_i = 1, i = 1, 2, \ldots, M_c - 1 \end{aligned} \tag{23}$$

where $\boldsymbol{Q}$ is given by

$$\boldsymbol{Q} = (\hat{\boldsymbol{E}}_{\mathrm{S}_2}\hat{\boldsymbol{E}}_{\mathrm{S}_2}^H)^T \circ \boldsymbol{P}_{\mathrm{S}_1} \tag{24}$$

and $\boldsymbol{P}_{\mathrm{S}_1} = \boldsymbol{I} - \hat{\boldsymbol{E}}_{\mathrm{S}_1}(\hat{\boldsymbol{E}}_{\mathrm{S}_1}^H\hat{\boldsymbol{E}}_{\mathrm{S}_1})^{-1}\hat{\boldsymbol{E}}_{\mathrm{S}_1}^H$. Note that the formulation in (23) is derived based on the setting that the first M_c sensors are calibrated. In fact, it can be applied to any partly calibrated ULAs with arbitrary placements of the calibrated sensors, provided that there is at least one pair of consecutive calibrated sensors. For instance, if the kth and $(k+1)$th sensors are calibrated, then the constraint in (23) should be replaced by $\overline{\gamma}_k = 1$.

We now proceed to solve the optimization problem in (23) and estimate the DOAs and the unknown gains and phases using the Lagrange multiplier method. First, we note that the constraint in (23) can be represented as

$$\boldsymbol{W}^H\overline{\boldsymbol{\gamma}} = \mathbf{1}_{M_c-1} \tag{25}$$

where $\boldsymbol{W}$ is an $(M-1)\times(M_c-1)$ matrix given by

$$\boldsymbol{W} = \begin{bmatrix} \boldsymbol{I}^{(M_c-1)\times(M_c-1)} \\ \mathbf{0}^{(M-M_c)\times(M_c-1)} \end{bmatrix}. \tag{26}$$

Hence, the problem can be rewritten as

$$\begin{aligned} \min_{\overline{\boldsymbol{\gamma}}} \quad & \overline{\boldsymbol{\gamma}}^H \boldsymbol{Q} \overline{\boldsymbol{\gamma}} \\ \text{s. t.} \quad & \boldsymbol{W}^H \overline{\boldsymbol{\gamma}} = \mathbf{1}_{M_c - 1}. \end{aligned} \tag{27}$$

To solve this problem using the Lagrange multiplier method, we form the Lagrangian function associated with (27) as follows

$$L(\overline{\boldsymbol{\gamma}}, \boldsymbol{\mu}) = \overline{\boldsymbol{\gamma}}^H \boldsymbol{Q} \overline{\boldsymbol{\gamma}} + \boldsymbol{\mu}^H (\boldsymbol{W}^H \overline{\boldsymbol{\gamma}} - \mathbf{1}_{M_c - 1}) \tag{28}$$

where $\boldsymbol{\mu}$ is the Lagrange multiplier. By setting the partial derivative of (28) with respect to $\overline{\boldsymbol{\gamma}}$ to zero, one gets the first-order necessary condition for optimality as $2\boldsymbol{Q}\overline{\boldsymbol{\gamma}} + \boldsymbol{W}\boldsymbol{\mu} = \mathbf{0}$, which leads to the optimal solution

$$\hat{\overline{\boldsymbol{\gamma}}} = \frac{1}{2} \boldsymbol{Q}^{-1} \boldsymbol{W} \boldsymbol{\mu}. \tag{29}$$

By substituting (29) back to the constraint (27), one can determine the Lagrange multiplier $\boldsymbol{\mu}$, and hence the final solution to (29) as follows:

$$\hat{\overline{\boldsymbol{\gamma}}} = \boldsymbol{Q}^{-1} \boldsymbol{W} (\boldsymbol{W}^H \boldsymbol{Q}^{-1} \boldsymbol{W})^{-1} \mathbf{1}_{M_c - 1}. \tag{30}$$

Consequently, the matrix $\boldsymbol{\Psi}$, DOAs $\{\theta_l\}_{l=1}^{L}$, gains $\{\rho_k\}_{k=1}^{M-M_c}$ and phases $\{\varphi_k\}_{k=1}^{M-M_c}$ can be estimated according to (19), (20), and (22).

It should be noted that a sufficient condition for the existence of (30) is that $\boldsymbol{Q}$ is nonsingular. However, in the infinite samples case, $\boldsymbol{Q}$ is singular. One possible way to handle this problem is to employ diagonal loading as suggested in [17], [24], [26], and [27]. More precisely, a small multiple of the identity matrix is added to $\boldsymbol{Q}$ to form the diagonally loaded matrix $\boldsymbol{Q}_{\mathrm{DL}} = \boldsymbol{Q} + \delta \boldsymbol{I}$. It is worth noting that in these robust algorithms, especially robust beamforming algorithms discussed in [26] and [27], the loading level δ is usually required to be optimally selected. Fortunately, in our case, we only require $\boldsymbol{Q}$ being nonsingular, and hence δ can be chosen as a small value. In fact, a large δ may degrade the accuracy of estimating $\overline{\boldsymbol{\gamma}}$ as well as other unknown parameters. Moreover, it is found by extensive experiments that, in finite sample cases, the matrix $\boldsymbol{Q}$ is always nonsingular, and hence there is no need for diagonal loading in general.

IV. Comparisons and Cramér–Rao Bounds

A. Comparisons

From the derivation in the previous section, it can be seen that the proposed method is similar to the conventional ESPRIT algorithm. Therefore, it is computationally efficient since the DOAs as well as the gains and phases can be estimated from (19) and (20) at the cost of an EVD, and no spectral search is required. Compared to ESPRIT, a more general case of partly calibrated ULAs is tackled. In [22], a root-RARE estimator was developed for partly calibrated subarray-based arrays with unknown vector translations. Since it generalizes the conventional root-MUSIC algorithm, it can be directly applied to fully calibrated ULAs. However, its extension to the case of partly calibrated ULAs is not straightforward. On the other hand, the spectral-RARE estimator derived in [24] allows the array geometry to be arbitrary, and it can be directly applied to the partly calibrated ULAs by letting the first M_c calibrated sensors be the first subarray and the other $M - M_c$ subarrays be of a single sensor. Therefore, the total number of subarrays is $M - M_c + 1$. According to the spectral-RARE estimator, the sensor number M, subarray number $M - M_c + 1$, and source number L must satisfy $M - M_c + 1 \leq M - L$, i.e.,

$$M_c \geq L + 1. \tag{31}$$

This indicates that the number of calibrated sensors in a ULA should be larger than the source number. For instance, the calibrated sensors in a ULA should be no less than four when the sources number is three. As a result, this method is not applicable when $M_c \leq L$. However, in the proposed method, we only require the number of calibrated sensors to be no less than two. In fact, this is the basic property of a partly calibrated ULA because when there are no calibrated sensors in a ULA, the array should be an uncalibrated rather than partly calibrated one. A number of works have studied the problem of sensor array processing with uncalibrated arrays [10]–[16]. For instance, an ESPRIT-based technique has been proposed for spatial signature matrix, but not DOA estimation with uncalibrated ULAs, in [16]. Different from this method, in our proposed method, we aim to estimate the DOAs as well as unknown array gains and phase in closed form by taking advantage of the calibrated sensors.

A special case of the proposed method occurs when the ULA is fully calibrated, i.e., $M_c = M$. In this case, we have $\boldsymbol{\gamma} = \boldsymbol{\rho} \circ \boldsymbol{\varphi} = \mathbf{1}_M$ and $\boldsymbol{\Gamma}(\overline{\boldsymbol{\gamma}}) = \boldsymbol{I}$. Consequently, the constrained problem in (21) is reduced to an unconstrained problem as follows:

$$\min_{\boldsymbol{\Psi}} ||\hat{\boldsymbol{E}}_{\mathrm{S}_2} - \hat{\boldsymbol{E}}_{\mathrm{S}_1} \boldsymbol{\Psi}||_{\mathrm{F}}^2 \tag{32}$$

and its solution is given by

$$\hat{\boldsymbol{\Psi}} = (\hat{\boldsymbol{E}}_{\mathrm{S}_1}^H \hat{\boldsymbol{E}}_{\mathrm{S}_1})^{-1} \hat{\boldsymbol{E}}_{\mathrm{S}_1}^H \hat{\boldsymbol{E}}_{\mathrm{S}_2}. \tag{33}$$

Apparently, this is the solution of the conventional ESPRIT algorithm. In other words, the proposed method can be regarded as a generalized version of the conventional ESPRIT algorithm. It is interesting to note that another generalized version of the ESPRIT algorithm has been studied in [25]. Different from our proposed method, this method is proposed to deal with arrays where any sensor of the first subarray and the corresponding sensor of the second subarray are displaced by different displacement vectors.

B. Cramér–Rao Bounds

In this section, closed-form expressions for the CRBs of partly calibrated ULAs with N zero mean and statistically independent Gaussian random vectors are given. The unknown vectors of DOAs $\boldsymbol{\theta}$, gains $\boldsymbol{g}$, and phases $\boldsymbol{p}$ are given by $\boldsymbol{\theta} = [\theta_1, \theta_2, \ldots, \theta_L]^T$, $\boldsymbol{g} = [\rho_1, \rho_2, \ldots, \rho_{M-M_c}]^T$, and

$\boldsymbol{p} = [\varphi_1, \varphi_2, , \ldots, \varphi_{M-M_c}]^T$, respectively. The CRB for DOA estimation is given by [10], [19]

$$\mathrm{CRB}(\boldsymbol{\theta}) = \frac{1}{2N} \times \{\mathrm{Re}[(\boldsymbol{S}\overline{\boldsymbol{A}}^H\boldsymbol{R}^{-1}\overline{\boldsymbol{A}}\boldsymbol{S}) \circ (\dot{\overline{\boldsymbol{A}}}^H\boldsymbol{R}^{-1}\dot{\overline{\boldsymbol{A}}})^T + (\boldsymbol{S}\overline{\boldsymbol{A}}^H\boldsymbol{R}^{-1}\dot{\overline{\boldsymbol{A}}}) \circ (\boldsymbol{S}\overline{\boldsymbol{A}}^H\boldsymbol{R}^{-1}\dot{\overline{\boldsymbol{A}}})^T]\}^{-1} \quad (34)$$

where $\mathrm{Re}\{x\}$ denotes the real part of x and

$$\dot{\overline{\boldsymbol{A}}} = \sum_{l=1}^{L} \frac{\partial \overline{\boldsymbol{A}}}{\partial \theta_l} = \boldsymbol{\Gamma}(\boldsymbol{\gamma}) \sum_{l=1}^{L} \frac{\partial \boldsymbol{A}}{\partial \theta_l} \quad (35)$$

since $\overline{\boldsymbol{A}} = \boldsymbol{\Gamma}(\boldsymbol{\gamma})\boldsymbol{A}$. The CRB for the gain estimation is given by [19]

$$\mathrm{CRB}(\boldsymbol{g}) = \frac{1}{2N}\{\mathrm{Re}\{\boldsymbol{H}[(\boldsymbol{P}\boldsymbol{A}\boldsymbol{S}\overline{\boldsymbol{A}}^H\boldsymbol{R}^{-1}) \circ (\boldsymbol{P}\boldsymbol{A}\boldsymbol{S}\overline{\boldsymbol{A}}^H\boldsymbol{R}^{-1})^T + (\boldsymbol{P}\boldsymbol{A}\boldsymbol{S}\overline{\boldsymbol{A}}^H\boldsymbol{R}^{-1}\overline{\boldsymbol{A}}\boldsymbol{S}\boldsymbol{A}^H\boldsymbol{P}^H) \circ (\boldsymbol{R}^{-1})^T]\boldsymbol{H}^T\}^{-1} \quad (36)$$

where $\boldsymbol{P} = \mathrm{diag}\{\boldsymbol{\varphi}\} = \mathrm{diag}\{\boldsymbol{1}_{M_c}^T, e^{j\varphi_1}, \ldots, e^{j\varphi_{M-M_c}}\}$ and $\boldsymbol{H}$ is an $(M - M_c) \times M$ matrix with its (m, n)th entry being

$$[\boldsymbol{H}]_{m,n} = \begin{cases} 1, & \text{if } n = M_c + m \\ 0, & \text{otherwise.} \end{cases} \quad (37)$$

Based on the derivations of CRBs for phase estimation of uncalibrated ULAs in [10] and gain estimation of partly calibrated ULAs in [19], the CRB for phase estimation of partly calibrated ULAs can be similarly derived and given by

$$\mathrm{CRB}(\boldsymbol{p}) = \frac{1}{2N}\{\mathrm{Re}\{\boldsymbol{H}[(\overline{\boldsymbol{A}}\boldsymbol{S}\overline{\boldsymbol{A}}^H\boldsymbol{R}^{-1}\overline{\boldsymbol{A}}\boldsymbol{S}\overline{\boldsymbol{A}}^H) \circ (\boldsymbol{R}^{-1})^T - (\overline{\boldsymbol{A}}\boldsymbol{S}\overline{\boldsymbol{A}}^H\boldsymbol{R}^{-1}) \circ (\overline{\boldsymbol{A}}\boldsymbol{S}\overline{\boldsymbol{A}}^H\boldsymbol{R}^{-1})^T]\boldsymbol{H}^T\}^{-1}. \quad (38)$$

It should be noted that the unknown phases are modeled to be direction-dependent in [19] and direction-independent in this paper. Hence, the CRB for phase estimation given in (38) is different from that in [19].

V. Simulation Results

In order to evaluate the performance of the proposed method, computer simulation of a partly calibrated ULA with $M = 10$ sensors separated by half a wavelength was performed. In all examples, the unknown gain and phase uncertainties are considered to be direction-independent and time-invariant. Three uncorrelated narrowband signals with identical power impinge on the array from the far field, and hence $L = 3$. The DOAs of them are assumed to be $-10°$, $10°$, and $20°$, respectively. The background noise is assumed to be AWGN.

A. Example I

In the first example, the first five sensor are assumed to be calibrated, i.e., $M_c = 5$, while the last five sensors are uncalibrated with unknown gain and phase uncertainties given by $0.8e^{j\pi/5}$, $1.25e^{-j\pi/3}$, $1.53e^{-j\pi/5}$, $0.75e^{j\pi/4}$, and $1.36e^{-j\pi/10}$.

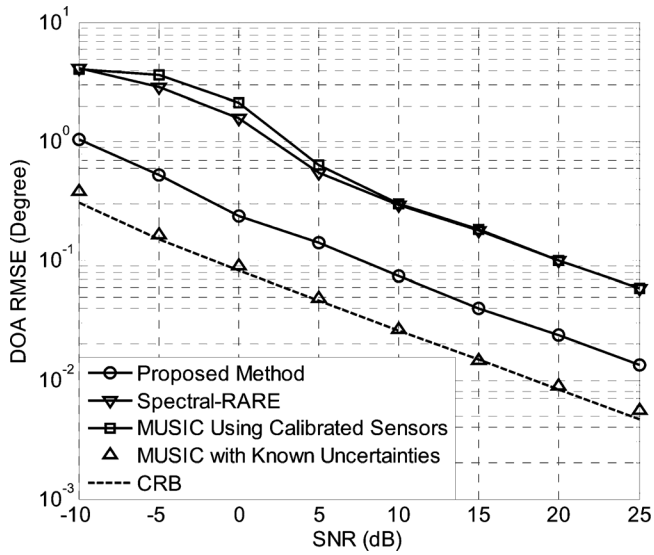

Fig. 1. RMSE of DOA estimation versus SNR. The number of snapshots $N = 500$, and the number of calibrated sensors $M_c = 5$.

At first, the performance of the proposed method is evaluated at different SNRs. The determinant-based spectral-RARE algorithm [24] was also tested for comparison. Moreover, the results of MUSIC using the first five calibrated sensors and MUSIC using the whole array with known uncertainties were also obtained. A total of 200 Monte Carlo experiments are run at each SNR, and the number of snapshots in each experiment is $N = 500$. The following root mean squared error (RMSE) of DOA estimation is used as the performance measure:

$$\mathrm{RMSE}_\theta = \sqrt{\frac{1}{KL}\sum_{k=1}^{K}\sum_{l=1}^{L}(\hat{\theta}_{k,l} - \theta_l)^2}$$

where K is the number of Monte Carlo experiments, and $\hat{\theta}_{k,l}$ is the estimated DOA of the lth signal in the kth experiment. In all examples, we let $K = 200$.

In Fig. 1, the RMSEs of the DOA estimates obtained by different methods versus SNR are compared, and the CRB is also displayed. Overall, it can be seen that, in the cases of partly calibrated ULAs, the proposed method can give better performance than the spectral-RARE algorithm and the MUSIC algorithm using the calibrated sensors. Moreover, it can be noted that the RMSEs of DOA estimated by all methods, except MUSIC with known uncertainties, cannot reach the CRB even at large SNRs. One possible explanation is that the performances of these methods are significantly dependent on the number of calibrated sensors. This will be shown in the last example, where we can see that the performances of these methods will be greatly improved with increasing number of calibrated sensors M_c. For example, for a large M_c, the RMSEs are close to the CRB even when the SNR is 5 dB.

Fig. 2 shows the success probability of DOA estimation. Here, the success probability is defined as N_S/K, where N_S is the number of experiments in which all of the

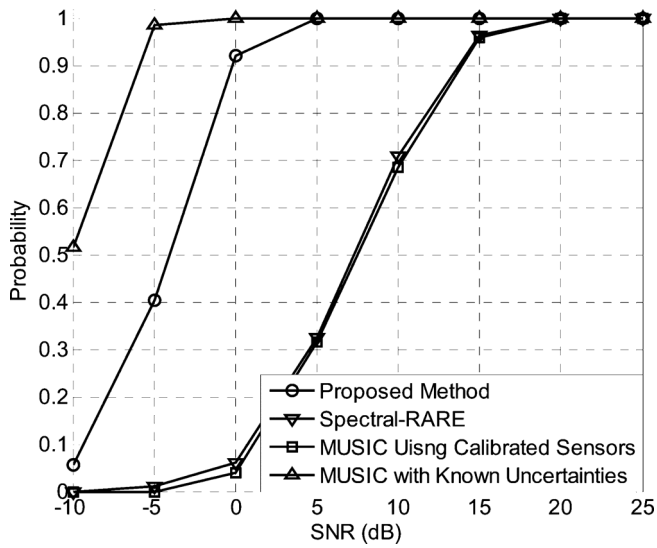

Fig. 2. Success probability of DOA estimation versus SNR. The number of snapshots $N = 500$, and the number of calibrated sensors $M_c = 5$.

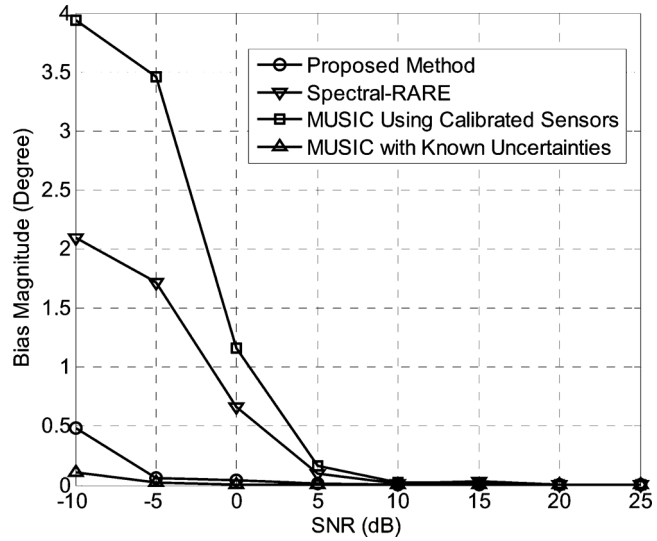

Fig. 3. Bias magnitude of DOA estimation of the third signal versus SNR. The number of snapshots $N = 500$, and the number of calibrated sensors $M_c = 5$.

DOA estimate bias magnitudes are smaller than 0.5°, i.e., $\max\{|\hat{\theta}_1 - \theta_1|, |\hat{\theta}_2 - \theta_2|, |\hat{\theta}_3 - \theta_3|\} \leq 0.5°$. Apparently, we notice that the proposed method can achieve the highest DOA estimation accuracy when the uncertainties are unknown. Even at low SNRs, the proposed method is able to successfully estimate all of the DOAs within the given bound with a high probability. This suggests that the proposed method is useful especially when the signals are seriously contaminated by noise.

Fig. 3 illustrates the magnitude of DOA estimation bias of the third signal, which is defined as $|K^{-1}\sum_{k=1}^{K}\hat{\theta}_{k,3} - \theta_3|$. We can find that even at a small SNR, the bias magnitude is rather small. When the SNR is larger than 0 dB, the estimation bias magnitude tends to be very small, whereas such a performance can only be obtained by the other methods with SNR larger than 10 dB.

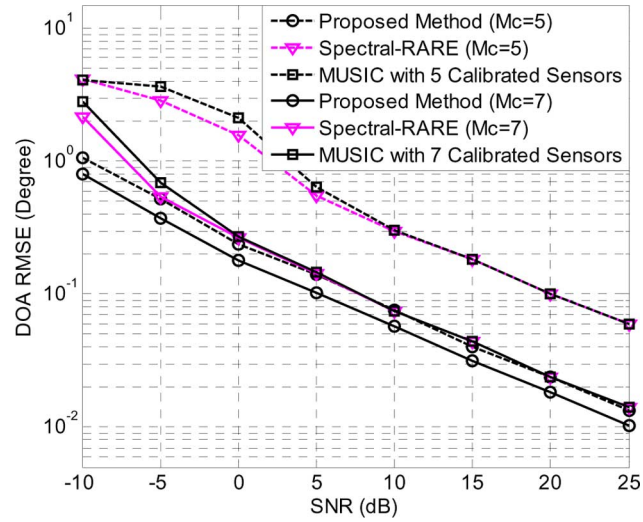

Fig. 4. RMSE of DOA estimation versus SNR. The number of snapshots $N = 500$, and the number of calibrated sensors $M_c = 5$ and $M_c = 7$.

TABLE I
ESTIMATED GAIN AND PHASE, BIAS MAGNITUDE, RMSE, AND CRB FOR THE FIRST UNCALIBRATED SENSOR AT DIFFERENT SNRS USING THE PROPOSED METHOD. TRUE VALUES ARE $\rho_1 = 0.8$ AND $\varphi_1 = 0.6283$(rad)

SNR (dB)	-10	-5	0	5	10	15	20
$\hat{\rho}_1$	0.9322	0.8435	0.8120	0.8011	0.8008	0.8002	0.8002
$\lvert\hat{\rho}_1 - \rho_1\rvert$	0.1322	0.0435	0.0120	0.0011	0.0008	0.0002	0.0002
RMSE_{ρ_1}	0.2274	0.0804	0.0346	0.0190	0.0099	0.0056	0.0034
CRB_{ρ_1}	0.0789	0.0388	0.0211	0.0118	0.0067	0.0038	0.0021
$\hat{\varphi}_1$	0.6421	0.6353	0.6327	0.6294	0.6291	0.6276	0.6284
$\lvert\hat{\varphi}_1 - \varphi_1\rvert$	0.0138	0.0070	0.0044	0.0011	0.0008	0.0007	0.0001
RMSE_{φ_1}	0.1857	0.0815	0.0393	0.0222	0.0125	0.0076	0.0039
CRB_{φ_1}	0.0986	0.0485	0.0263	0.0148	0.0083	0.0047	0.0026

In order to evaluate the performance of the proposed method in gain and phase estimation, the estimated gains and phases, bias magnitudes, and RMSEs are obtained by the proposed method with 200 experiments. The CRBs for gains and phases estimation are also calculated based on (36) and (38) for comparison. Table I shows the averaged gain and phase estimates, bias magnitude, RMSE, and CRB for the first uncalibrated sensor at different SNRs. Since the estimation results of the other four uncalibrated sensors obtained by the proposed method are similar to those of the first uncalibrated sensor, they are omitted for simplicity.

B. Example II

In this example, we will evaluate the effect of the number of calibrated sensors in a ULA on DOA estimation. First, we follow the settings in the previous example, but the calibrated sensors are assumed to be seven, i.e., $M_c = 7$. The unknown gains and phases of the uncalibrated sensors are identical to those in Example I, i.e., $1.53e^{-j\pi/5}$, $0.75e^{j\pi/4}$, and $1.36e^{-j\pi/10}$. Fig. 4 shows the RMSEs of DOA estimation when $M_c = 7$. Moreover, the results of $M_c = 5$ obtained in Example I are also displayed for comparison. It can be

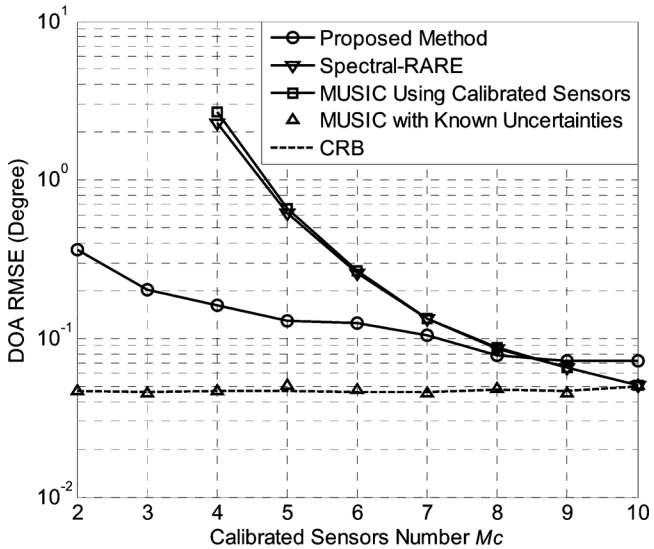

Fig. 5. The RMSE of DOA estimation versus the number of calibrated sensors M_c. The number of snapshots $N = 500$, the $\mathrm{SNR} = 5$ dB.

noted that the performances of the methods, especially the spectral-RARE algorithm and the MUSIC algorithm using calibrated sensors, are greatly improved by reducing the number of uncalibrated sensors.

Next, we set 5 dB to and the number of snapshots to $N = 500$ and evaluate the performance of the proposed method with different number of calibrated sensors. More precisely, the RMSE is calculated for $M_{\mathrm{c}} = 2, 3, \ldots, 10$. It should be noted that the gain and phase vector $\boldsymbol{\gamma}$ is chosen to be $\boldsymbol{\gamma} = [\mathbf{1}_{M_{\mathrm{c}}}^T, \boldsymbol{c}(M_{\mathrm{c}} - 1 : 8)]^T$ when there are M_{c} calibrated sensors, where $\boldsymbol{c}$ is defined as the following 1×8 vector:

$$\boldsymbol{c} = [0.88e^{j\pi/6}, 1.45e^{-j\pi/8}, 0.94e^{-j\pi/4}, 0.8e^{j\pi/5}, 1.25e^{-j\pi/3}, 1.53e^{-j\pi/5}, 0.75e^{j\pi/4}, 1.36e^{-j\pi10}].$$

Fig. 5 shows the RMSEs versus the number of calibrated sensors M_{c}. We remark here that both spectral-RARE and MUSIC using calibrated sensors are not applicable when the number of calibrated sensors is less than four, i.e., $M_{\mathrm{c}} < 4$, because these two algorithms require the number of calibrated sensors be larger than the number of sources in the case of ULA.

From Fig. 5, we can see that the performance of each method can be improved by increasing the number of calibrated sensors. It is worth noting that when the number of calibrated sensors is 10, i.e., the ULA is fully calibrated without imperfections, the proposed method will reduce to the conventional ESPRIT algorithm, whereas both the spectral-RARE algorithm and MUSIC using calibrated sensors will reduce to the conventional MUSIC algorithm. This is the reason why the spectral-RARE algorithm achieves a better performance when $M_{\mathrm{c}} = 10$.

VI. Conclusion

A new direction finding method for partly calibrated ULAs is presented. It extends the conventional ESPRIT algorithm by modeling imperfections of the ULAs as unknown gains and phases. For a fully calibrated array, the proposed method reduces to the conventional ESPRIT algorithm. The DOAs and unknown gains and phases can be estimated in closed form without performing a spectral search. Thus, the proposed method is computationally attractive. The CRBs of the partly calibrated ULAs are also presented. Simulation results show that the proposed method outperforms the conventional methods especially when the number of uncalibrated sensors is large, and satisfactory performance can be achieved even at low SNRs.

Appendix

In this appendix, we briefly give the derivation of the problem in (23).

Substituting (22) into (21), the objective function can be rewritten as

$$||\boldsymbol{\Gamma}(\overline{\boldsymbol{\gamma}})\hat{\boldsymbol{E}}_{\mathrm{S}_2} - \hat{\boldsymbol{E}}_{\mathrm{S}_1}\boldsymbol{\Psi}||_{\mathrm{F}}^2 = ||\boldsymbol{P}_{\mathrm{S}_1}\boldsymbol{\Gamma}(\overline{\boldsymbol{\gamma}})\hat{\boldsymbol{E}}_{\mathrm{S}_2}||_{\mathrm{F}}^2 \tag{39}$$

where $\boldsymbol{P}_{\mathrm{S}_1} = \boldsymbol{I} - \hat{\boldsymbol{E}}_{\mathrm{S}_1}(\hat{\boldsymbol{E}}_{\mathrm{S}_1}^H\hat{\boldsymbol{E}}_{\mathrm{S}_1})^{-1}\hat{\boldsymbol{E}}_{\mathrm{S}_1}^H$ is an $(M-1)\times(M-1)$ projection matrix. It is known that $||\boldsymbol{B}||_{\mathrm{F}}^2 = \mathrm{trace}\{\boldsymbol{B}^H\boldsymbol{B}\}$ and $\mathrm{trace}\{\boldsymbol{BC}\} = \mathrm{trace}\{\boldsymbol{CB}\}$ for any $(m \times n)$ matrix $\boldsymbol{B}$ and $(n \times m)$ matrix $\boldsymbol{C}$, then (39) can be rewritten as

$$\begin{aligned} ||\boldsymbol{P}_{\mathrm{S}_1}\boldsymbol{\Gamma}(\overline{\boldsymbol{\gamma}})\hat{\boldsymbol{E}}_{\mathrm{S}_2}||_{\mathrm{F}}^2 &= \mathrm{trace}\{\hat{\boldsymbol{E}}_{\mathrm{S}_2}^H\boldsymbol{\Gamma}^H(\overline{\boldsymbol{\gamma}})\boldsymbol{P}_{\mathrm{S}_1}^H\boldsymbol{P}_{\mathrm{S}_1}\boldsymbol{\Gamma}(\overline{\boldsymbol{\gamma}})\hat{\boldsymbol{E}}_{\mathrm{S}_2}\} \\ &= \mathrm{trace}\{\hat{\boldsymbol{E}}_{\mathrm{S}_2}\hat{\boldsymbol{E}}_{\mathrm{S}_2}^H\boldsymbol{\Gamma}^H(\overline{\boldsymbol{\gamma}})\boldsymbol{P}_{\mathrm{S}_1}\boldsymbol{\Gamma}(\overline{\boldsymbol{\gamma}})\} \end{aligned} \tag{40}$$

where the property $\boldsymbol{P}_{\mathrm{S}_1}^H\boldsymbol{P}_{\mathrm{S}_1} = \boldsymbol{P}_{\mathrm{S}_1}$ is utilized. Moreover, based on the following identity [28]:

$$\mathrm{trace}\{\boldsymbol{M}\boldsymbol{\Gamma}^H(\boldsymbol{d})\boldsymbol{N}\boldsymbol{\Gamma}(\boldsymbol{d})\} = \boldsymbol{d}^H(\boldsymbol{M}^T \circ \boldsymbol{N})\boldsymbol{d} \tag{41}$$

where $\boldsymbol{M}$ and $\boldsymbol{N}$ are $m \times m$ matrices, $\boldsymbol{d} = [d_1, d_2, \ldots, d_m]^T$, and $\boldsymbol{\Gamma}(\boldsymbol{d}) = diag\{d_1, d_2, \ldots, d_m\}$, the objective function (40) can be further simplified to

$$\mathrm{trace}\{\hat{\boldsymbol{E}}_{\mathrm{S}_2}\hat{\boldsymbol{E}}_{\mathrm{S}_2}^H\boldsymbol{\Gamma}^H(\overline{\boldsymbol{\gamma}})\boldsymbol{P}_{\mathrm{S}_1}\boldsymbol{\Gamma}(\overline{\boldsymbol{\gamma}})\} = \overline{\boldsymbol{\gamma}}^H\left((\hat{\boldsymbol{E}}_{\mathrm{S}_2}\hat{\boldsymbol{E}}_{\mathrm{S}_2}^H)^T \circ \boldsymbol{P}_{\mathrm{S}_1}\right)\overline{\boldsymbol{\gamma}}. \tag{42}$$

Hence, the problem in (21) becomes

$$\begin{aligned} \min_{\overline{\boldsymbol{\gamma}}} \quad & \overline{\boldsymbol{\gamma}}^H\left((\hat{\boldsymbol{E}}_{\mathrm{S}_2}\hat{\boldsymbol{E}}_{\mathrm{S}_2}^H)^T \circ \boldsymbol{P}_{\mathrm{S}_1}\right)\overline{\boldsymbol{\gamma}} \\ \text{s. t.} \quad & \overline{\gamma}_i = 1, i = 1, 2, \ldots, M_{\mathrm{c}} - 1 \end{aligned} \tag{43}$$

which is identical to (23).

Acknowledgment

The authors would like to thank the reviewers and editors for their useful comments and suggestions.

References

[1] H. Krim and M. Viberg, "Two decades of array signal processing research," *IEEE Signal Process. Mag.*, vol. 13, no. 4, pp. 67–95, Jul. 1996.

[2] E. Tuncer and B. Freidlander, "Calibration in array processing," in *Classical and Modern Direction-of-Arrival Estimation*. Amsterdam, The Netherlands: Elsevier, 2009.
[3] R. O. Schmidt, "Multiple emitter location and signal parameter estimations," *IEEE Trans. Antennas Propag.*, vol. AP-34, no. 3, pp. 276–280, Mar. 1986.
[4] A. J. Barabell, "Improving the resolution performance of eigenstructure-based direction-finding algorithms," in *Proc. ICASSP*, Boston, MA, May 1983, pp. 336–339.
[5] R. Roy and T. Kailath, "ESPRIT—Estimation of signal parameters via rotational invariance techniques," *IEEE Trans. Acoust., Speech, Signal Process.*, vol. 37, no. 7, pp. 984–995, Jul. 1989.
[6] P. Stoica and A. Nehorai, "MUSIC, maximum likelihood, and Cramer Rao bound," *IEEE Trans. Acoust., Speech, Signal Process.*, vol. 37, no. 5, pp. 720–741, May 1989.
[7] A. Swindlehurst and T. Kailath, "A performance analysis of subspace-based methods in the presence of model errors, part I: The MUSIC algorithm," *IEEE Trans. Signal Process.*, vol. 40, no. 7, pp. 1758–1773, Jul. 1992.
[8] A. Ferreol, P. Larzabal, and M. Viberg, "On the asymptotic performance analysis of subspace DOA estimation in the presence of modeling errors: Case of MUSIC," *IEEE Trans. Signal Process.*, vol. 54, no. 3, pp. 907–920, Mar. 2006.
[9] A. Ferreol, P. Larzabal, and M. Viberg, "On the resolution probability of MUSIC in presence of modeling errors," *IEEE Trans. Signal Process.*, vol. 56, no. 5, pp. 1945–1953, May 2008.
[10] B. Friedlander and A. J. Weiss, "Direction finding in the presence of mutual coupling," *IEEE Trans. Antennas Propag.*, vol. 39, no. 3, pp. 273–284, Mar. 1991.
[11] E. K. L. Hung, "A critical study of a self-calibration direction-finding method for arrays," *IEEE Trans. Signal Process.*, vol. 42, no. 2, pp. 471–474, Feb. 1994.
[12] B. C. Ng and C. M. S. See, "Sensor-array calibration using a maximum-likelihood approach," *IEEE Trans. Antennas Propag.*, vol. 44, no. 6, pp. 827–835, Jun. 1996.
[13] K. C. Ho and L. Yang, "On the use of a calibration emitter for source localization in the presence of sensor position uncertainty," *IEEE Trans. Signal Process.*, vol. 56, no. 12, pp. 5758–5772, Dec. 2008.
[14] Z. Ye, J. Dai, X. Xu, and X. Wu, "DOA estimation for uniform linear array with mutual coupling," *IEEE Trans. Aerosp. Electron. Syst.*, vol. 45, no. 1, pp. 280–288, Jan. 2009.
[15] X. Xu, Z. Ye, and Y. Zhang, "DOA estimation for mixed signals in the presence of mutual coupling," *IEEE Trans. Signal Process.*, vol. 57, no. 9, pp. 3523–3532, Sep. 2009.
[16] D. Astély, A. L. Swindlehurst, and B. Ottersten, "Spatial signature estimation for uniform linear arrays with unknown receiver gain and phases," *IEEE Trans. Signal Process.*, vol. 47, no. 8, pp. 2128–2138, Aug. 1999.
[17] S. Haykin and K. J. L. Ray, *Handbook on Array Processing and Sensor Networks*. Hoboken, NJ: Wiley, 2010.
[18] P. Stocia, M. Viberg, K. M. Wong, and Q. Wu, "Maximum-likelihood bearing estimation with partly calibrated arrays in spatially correlated noise field," *IEEE Trans. Signal Process.*, vol. 44, no. 4, pp. 888–899, Apr. 1996.
[19] A. J. Weiss and B. Friedlander, "DOA and steering vector estimation using a partially calibrated array," *IEEE Trans. Aerosp., Electron. Syst.*, vol. 32, no. 3, pp. 1047–1057, Jul. 1996.
[20] M. Li and Y. Lu, "Source bearing and steering-vector estimation using partially calibrated arrays," *IEEE Trans. Aerosp., Electron. Syst.*, vol. 45, no. 4, pp. 1361–1372, Oct. 2009.
[21] M. Pesavento, A. B. Gershman, and K. M. Wong, "Direction of arrival estimation in partly calibrated time-varying sensor arrays," in *Proc. ICASSP*, Salt Lake City, UT, May 2001, pp. 3005–3008.
[22] M. Pesavento, A. B. Gershman, and K. M. Wong, "Direction finding in partly-calibrated sensor arrays composed of multiple subarrays," *IEEE Trans. Signal Process.*, vol. 50, no. 9, pp. 2103–2115, Sep. 2002.
[23] C. M. S. See and A. B. Gershman, "Subspace-based direction finding in partly calibrated arrays of arbitrary geometry," in *Proc. ICASSP*, Orlando, FL, Apr. 2002, pp. 3013–3016.
[24] C. M. S. See and A. B. Gershman, "Direction-of-arrival estimation in partly calibrated subarray-based sensor arrays," *IEEE Trans. Signal Process.*, vol. 52, no. 2, pp. 329–338, Feb. 2004.
[25] F. Gao and A. B. Gershman, "A generalized ESPRIT approach to direction-of-arrival estimation," *IEEE Signal Process. Lett.*, vol. 12, no. 3, pp. 254–257, Mar. 2005.
[26] Y. Hua, A. Gershman, and Q. Cheng, *High-resolution and Robust Signal Processing*. New York: Marcel Dekker, 2003.
[27] J. Li and P. Stoica, *Robust Adaptive Beamforming*. Hoboken, NJ: Wiley, 2006.
[28] J. R. Magnus and H. Neudecker, "Mathematical preliminaries," in *Matrix Differential Calculus with Applications in Statistics and Econometrics*, 2nd ed. New York: Wiley, 1999.

Bin Liao (S'09) received the B.Eng. and M.Eng. degrees from Xidian University, Xi'an, China, in 2006 and 2009, respectively, and is currently pursuing the Ph.D. degree in electrical and electronic engineering at the University of Hong Kong, Hong Kong.

His main research interests are array signal processing and adaptive filtering.

Shing Chow Chan (S'87–M'92) received the B.S. (Eng.) and Ph.D. degrees from the University of Hong Kong, Hong Kong, in 1986 and 1992, respectively.

Since 1994, he has been with the Department of Electrical and Electronic Engineering, University of Hong Kong, and is now a Professor. He held visiting positions with Microsoft Corporation, Redmond, WA; Microsoft Research Asia, Beijing, China; University of Texas at Arlington; and Nanyang Technological University, Singapore. His research interests include fast transform algorithms, filter design and realization, multirate and array signal processing, communications and biomedical signal processing, and image-based rendering.

Dr. Chan is currently a member of the Digital Signal Processing Technical Committee of the IEEE Circuits and Systems Society and an Associate Editor of the *Journal of Signal Processing Systems*. He was an Associate Editor of the IEEE TRANSACTIONS ON CIRCUITS AND SYSTEMS—I: REGULAR PAPERS from 2008 to 2009, and Chairman of the IEEE Hong Kong Chapter of Signal Processing from 2000 to 2002.